



Triply heavy tetraquark states: masses and other properties

Zhen-Hui Zhu^{1,a}, Wen-Xuan Zhang^{1,b}, DuoJie Jia^{1,2,c}

¹ Institute of Theoretical Physics, College of Physics and Electronic Engineering, Northwest Normal University, Lanzhou 730070, China

² Lanzhou Center for Theoretical Physics, Lanzhou University, Lanzhou 730000, China

Received: 28 November 2023 / Accepted: 20 March 2024
© The Author(s) 2024

Abstract In this work, we study masses and other static properties of triply heavy tetraquarks in the unified framework of the MIT bag which incorporates chromomagnetic interactions and enhanced binding energy. The masses, magnetic moments and charge radii of all strange and nonstrange (ground) states of triply heavy tetraquarks are computed, suggesting that all of triply heavy tetraquarks are above the respective two-meson thresholds. We also estimate relative decay widths of main decay channels of two-heavy mesons for these tetraquarks.

1 Introduction

Study of exotic multi-quark states and hadronic molecules has been an interesting topic and continuous attention since the observation of the charmonium like state $X(3872)$ in 2003 whose quantum number was later shown to be $J^P = 1^{++}$ [1]. Since then, a large number of XYZ states were discovered experimentally, such as the charmonium-like states $Z_c(3885)$ [2,3], the $Z_c(4020)$ [4], the $Z_c(4025)$ [3], the $Z_{cs}(3985)$ [5], the $Z_{cs}(4000)$ [6], the $Z_c(4200)$ [7] and the $Z_c(4430)$ [8], many of which are possible candidates of multi-quark state or hadronic molecule [9,10]. Some of the observed XYZ states, like the charged state $Z_c(3900)$ [11,12], are undoubtedly exotic. In 2020, the first fully charm tetraquark, the $X(6900)$, has been observed by LHCb in the di- J/Ψ invariant masses spectrum [13]. In 2021, the first doubly charmed tetraquark T_{cc}^{++} was discovered in experiment [14]. If these states are confirmed to be exotic, they may be the candidates of tetraquarks. Many theoretical discussions exist for the tetraquarks and multi-quarks with different approaches [15–23]. For the review see Refs. [24–37].

^a e-mail: ZhuzH88@outlook.com

^b e-mail: zhangwx89@outlook.com

^c e-mail: jiadj@nwnu.edu.cn (corresponding author)

There exist several approaches devoted to triply heavy tetraquark states, such as AdS/QCD potential [38], the quark models [39–41] and the chromomagnetic interaction model [42,43,46]. In the discussions, the method of the MIT bag model is rarely employed to explore triply heavy tetraquarks though it is successful for light hadrons. Main reason may be that the conventional MIT bag model fails to apply to heavy hadrons where some extra binding energy, vanishing between light quarks (u/d and s), enters between heavy quarks (c and b) and between heavy and strange quarks [37] and are necessary to reconcile light flavor dynamics with heavy flavor dynamics within a unified bag model [45]. When the chromomagnetic interaction added which has two different mass scales (one light mass scale and one heavy mass scale), the strong coupling $\alpha_s(R)$ tends to favor running with the bag radii R in order to correctly describe mass splittings of hadrons [45]. This makes it involving to explore the heavy hadrons like heavy tetraquarks in which two heavy quarks (or more) or heavy and strange quarks are involved using the bag picture like the MIT bag model.

In this work, we apply the MIT bag model [44,45] which incorporate the chromomagnetic interaction and enhanced binding energy between heavy flavors to calculate the masses, magnetic moments and charge radii for all ground (strange and nonstrange) states of triply heavy tetraquarks. The dynamical computation indicates that all of triply heavy tetraquarks are above the respective two-meson thresholds. By the way, we estimate the main decay widths of two-heavy mesons for these triply heavy tetraquarks.

This paper will be organized as follows. In Sect. 2, we briefly review the MIT bag model that we use in this work. We present the color-spin wave functions for tetraquark states in details also in this section. In Sect. 3, computation is given for the masses and other properties for the triply heavy tetraquarks. The paper ends with summary in Sect. 4.

2 The MIT bag model with binding energy

2.1 Mass formula

The MIT bag model assumes hadron to be a spherical bag(with the radii R) with quarks confined in it. The mass formula which includes the enhanced binding energy E_B and chromomagnetic interactions(CMI) can be written as [44]

$$\left\{ \begin{array}{l} m_n = 0, \quad m_s = 0.279 \text{ GeV}, \quad m_c = 1.641 \text{ GeV}, \quad m_b = 5.093 \text{ GeV}, \\ Z_0 = 1.83, \quad B^{1/4} = 0.145 \text{ GeV}, \quad \alpha_s = 0.55. \end{array} \right\} \tag{7}$$

$$\left\{ \begin{array}{l} B_{cs} = -0.025 \text{ GeV}, \quad B_{cc} = -0.077 \text{ GeV}, \quad m_{bs} = -0.032 \text{ GeV}, \\ B_{bb} = -0.128 \text{ GeV}, \quad B_{bc} = -0.101 \text{ GeV}. \end{array} \right\} \tag{8}$$

$$M(R) = \sum_{i=1}^4 \omega_i + \frac{4}{3} \pi R^3 B - \frac{Z_0}{R} + E_B + \langle \Delta H \rangle, \tag{1}$$

$$\omega_i = \left(m_i^2 + \frac{x_i^2}{R^2} \right)^{1/2}, \tag{2}$$

The first three terms contain the kinetic energy of all quarks, the volume energy with bag constant B and the zero-point energy with coefficient Z_0 . The total binding energy $E_B = \sum_{I < J} B_{IJ}$ stands for the sum of the enhanced binding energies B_{IJ} between the I and J quarks. The last term $M_{CMI} = \langle \Delta H \rangle$ is the chromomagnetic interaction among quarks within bag, given by

$$M_{CMI} = - \sum_{i < j} (\lambda_i \cdot \lambda_j) (\sigma_i \cdot \sigma_j) C_{ij}, \tag{3}$$

where λ_i is the Gell-Mann matrices in color space, σ_i is the Pauli matrices in spin space and C_{ij} the CMI parameters, given by

$$C_{ij} = 3 \frac{\alpha_s(R)}{R^3} \bar{\mu}_i \bar{\mu}_j I_{ij}, \tag{4}$$

$$\bar{\mu}_i = \frac{R}{6} \frac{4\omega_i R + 2m_i R - 3}{2\omega_i R (\omega_i R - 1) + m_i R}, \tag{5}$$

$$I_{ij} = 1 + 2 \int_0^R \frac{dr}{r^4} \bar{\mu}_i \bar{\mu}_j = 1 + F(x_i, x_j). \tag{6}$$

Here, $\bar{\mu}_i$ is reduced magnetic moment, $F(x_i, x_j)$ a rational function and $\alpha(R)$ the strong coupling, all of which are detailed in Appendix A, where two relations relations for $F(x_i, x_j)$ and $\alpha(R)$ of computing the CMI matrix elements is also given.

The binding energy B_{IJ} stems mainly from the short-range chromoelectric interaction between heavy quark I and/or antiquark J , which is greatly enhanced compared to that between light quarks. Since the later is much small, it can be ignored. In the case that the quark (I) is heavy and the other quark (J) is strange, we assume B_{IJ} to be nonva-

nishing, as assumed in Refs. [37,45]. As such, for the color configuration $\bar{\mathbf{3}}_c$ of the quark pair, there exist five binding energies: $B_{cs}, B_{cc}, B_{bs}, B_{bb}$ and B_{bc} .

For the other parameters like quark masses, zero-point energy Z_0 in Eqs. (1) and (2) except for B_{IJ} , we apply the following input values [44,45]. For the binding energy between quark pairs ij in the rep. $\bar{\mathbf{3}}_c$, we employ the values from Ref. [45]:

In computation, we solve the transcendental equation (A3) interactively to find x_i depending on R . Here, the bag radii R varies with hadrons and can be solved numerically by Eq. (1) using variational method provided that the CMI matrix is evaluated for a given configuration of tetraquark wavefunction, which we address in the following.

2.2 The color-spin wavefunction

In this subsection we present the color-spin wavefunctions of all triply heavy tetraquark states which are required to evaluate the CMI mass splitting due to the chromomagnetic interaction in Eq. (3). For simplicity, we express the flavor parts of the tetraquarks explicitly in terms of the quark flavors($n = u/d, s, c$ and b). For the colorless tetraquark T , its color wavefunction has two color structure $\mathbf{6}_c \otimes \bar{\mathbf{6}}_c$ or $\bar{\mathbf{3}}_c \otimes \mathbf{3}_c$ in the notation of the color representations $3_c(\bar{3}_c)$ and $6_c(\bar{6}_c)$, corresponding to the following color configurations

$$\phi_1^T = \left| (q_1 q_2)^6 (\bar{q}_3 \bar{q}_4)^{\bar{6}} \right\rangle, \quad \phi_2^T = \left| (q_1 q_2)^{\bar{3}} (\bar{q}_3 \bar{q}_4)^3 \right\rangle, \tag{9}$$

respectively. For the spin part of tetraquark wavefunction, there are six configurations (spin bases in spin space)

$$\begin{aligned} \chi_1^T &= \left| (q_1 q_2)_1 (\bar{q}_3 \bar{q}_4)_2 \right\rangle, & \chi_2^T &= \left| (q_1 q_2)_1 (\bar{q}_3 \bar{q}_4)_1 \right\rangle, \\ \chi_3^T &= \left| (q_1 q_2)_1 (\bar{q}_3 \bar{q}_4)_1 \right\rangle_0, & \chi_4^T &= \left| (q_1 q_2)_1 (\bar{q}_3 \bar{q}_4)_0 \right\rangle_1, \\ \chi_5^T &= \left| (q_1 q_2)_0 (\bar{q}_3 \bar{q}_4)_1 \right\rangle_1, & \chi_6^T &= \left| (q_1 q_2)_0 (\bar{q}_3 \bar{q}_4)_0 \right\rangle_0. \end{aligned} \tag{10}$$

Combining the color and spin parts of wavefunctions, tetraquark has twelve wavefunctions in their ground(1S) state,

$$\begin{aligned} \phi_1^T \chi_1^T &= \left| (q_1 q_2)_1^6 (\bar{q}_3 \bar{q}_4)_1^{\bar{6}} \right\rangle_2 \delta_{12}^A \delta_{34}^A, \\ \phi_2^T \chi_1^T &= \left| (q_1 q_2)_1^{\bar{3}} (\bar{q}_3 \bar{q}_4)_1^3 \right\rangle_2 \delta_{12}^S \delta_{34}^S, \\ \phi_1^T \chi_2^T &= \left| (q_1 q_2)_1^6 (\bar{q}_3 \bar{q}_4)_1^{\bar{6}} \right\rangle_1 \delta_{12}^A \delta_{34}^A, \\ \phi_2^T \chi_2^T &= \left| (q_1 q_2)_1^{\bar{3}} (\bar{q}_3 \bar{q}_4)_1^3 \right\rangle_1 \delta_{12}^S \delta_{34}^S, \end{aligned}$$

$$\begin{aligned}
 \phi_1^T \chi_3^T &= \left| (q_1 q_2)_1^6 (\bar{q}_3 \bar{q}_4)_1^6 \right\rangle_0 \delta_{12}^A \delta_{34}^A, \\
 \phi_2^T \chi_3^T &= \left| (q_1 q_2)_1^3 (\bar{q}_3 \bar{q}_4)_1^3 \right\rangle_0 \delta_{12}^S \delta_{34}^S, \\
 \phi_1^T \chi_4^T &= \left| (q_1 q_2)_1^6 (\bar{q}_3 \bar{q}_4)_0^6 \right\rangle_1 \delta_{12}^A \delta_{34}^S, \\
 \phi_2^T \chi_4^T &= \left| (q_1 q_2)_1^3 (\bar{q}_3 \bar{q}_4)_0^3 \right\rangle_1 \delta_{12}^S \delta_{34}^A, \\
 \phi_1^T \chi_5^T &= \left| (q_1 q_2)_0^6 (\bar{q}_3 \bar{q}_4)_1^6 \right\rangle_1 \delta_{12}^S \delta_{34}^A, \\
 \phi_2^T \chi_5^T &= \left| (q_1 q_2)_0^3 (\bar{q}_3 \bar{q}_4)_1^3 \right\rangle_1 \delta_{12}^A \delta_{34}^S, \\
 \phi_1^T \chi_6^T &= \left| (q_1 q_2)_0^6 (\bar{q}_3 \bar{q}_4)_0^6 \right\rangle_0 \delta_{12}^S \delta_{34}^S, \\
 \phi_2^T \chi_6^T &= \left| (q_1 q_2)_0^3 (\bar{q}_3 \bar{q}_4)_0^3 \right\rangle_0 \delta_{12}^A \delta_{34}^A.
 \end{aligned} \tag{11}$$

where the δ is defined to take flavor symmetry into account when writing tetraquark wavefunction. Firstly, $\delta_{12}^S = 0$ ($\delta_{12}^A = 0$) if two quarks q_1 and q_2 are antisymmetric (symmetric) in flavor space; Secondly, $\delta_{34}^A = 0$ ($\delta_{34}^S = 0$) if q_3 and q_4 are symmetric (antisymmetric) in flavor space; Thirdly, $\delta_{12}^S = \delta_{12}^A = 1$ and $\delta_{34}^S = \delta_{34}^A = 1$ in all other cases.

For given color configurations one can write binding energy explicitly $E_B = \sum_{I < J} B_{IJ} = \sum_{I < J} g_{IJ} B_{IJ}(\bar{3}_c)$ with the help of the ratios g_{IJ} of the color factor $\langle \lambda_I \cdot \lambda_J \rangle$ for given quark pair $q_I q_J$ relative to the color factor $\langle \lambda_I \cdot \lambda_J \rangle_{\bar{3}_c}$ for the quark pair $q_I q_J$ in the color antitriplet ($\bar{3}_c$), provided that the binding energy linearly scales with this factor. In the case of quark pairs in the color antitriplet $\bar{3}_c$ and singlet 1_c , this is known as the 1/2-rule the short-range interaction: $B([qq']_{3_c}) = (1/2)B([qq']_{1_c})$. For the tetraquark with color configuration $\phi_1^T = \left| (q_1 q_2)^6 (\bar{q}_3 \bar{q}_4)^6 \right\rangle$, one can compute scaling ratios g_{IJ} [45] for each pair $q_I q_J$ in tetraquark $(q_1 q_2) (\bar{q}_3 \bar{q}_4)$ and find the scaled binding energy $g_{IJ} B_{IJ}(\bar{3}_c)$, giving raised to total binding energy,

$$\begin{aligned}
 E_B(\phi_1^T) &= -\frac{1}{2}B_{12} + \frac{5}{4}B_{13} + \frac{5}{4}B_{14} + \frac{5}{4}B_{23} \\
 &\quad + \frac{5}{4}B_{24} - \frac{1}{2}B_{34}.
 \end{aligned} \tag{12}$$

Similarly, for the tetraquark with color configuration $\phi_2^T = \left| (q_1 q_2)^3 (\bar{q}_3 \bar{q}_4)^3 \right\rangle$, the total binding energy is found to be [45]

$$E_B(\phi_2^T) = B_{12} + \frac{1}{2}B_{13} + \frac{1}{2}B_{14} + \frac{1}{2}B_{23} + \frac{1}{2}B_{24} + B_{34}, \tag{13}$$

where $B_{ij} = B_{ij}(\bar{3}_c)$ stands for the enhanced binding energy between quark i and j in $\bar{3}_c$, which are nonvanishing only between heavy quarks or between heavy quarks and strange quarks. Here, the numeric prefactors in front of B_{ij} are the color factor ratios g_{ij} of the quark pair (i, j) in given configurations $\phi_{1,2}^T$. In the case of the quark pair 12 in 6_c in the state

ϕ_1^T , for instance, the color factor ratio is $-1 : 2$ relative to that in $\bar{3}_c$, and that for the pair 13 the ratio is $5 : 4$ relative to that in $\bar{3}_c$. For the details of the color factors and their ratios [45], see Appendix B.

Notice that in the color representation $\bar{3}_c$, the binding energy for the given flavor of the quark pairs ij can be obtained from Ref. [45].

For the color or spin matrices between quarks in given tetraquark with wavefunctions $\phi_{1,2}^T$, one can employ the respective matrix formula (B1) and (B2) in Appendix B. For tetraquarks with wavefunction bases (ϕ_1^T, ϕ_2^T) , the color factor matrices are given explicitly in Appendix B.

Using the CG coefficients for the given tetraquark configurations $\phi_{1,2}^T$, one can write the six spin wavefunctions explicitly. They are

$$\begin{aligned}
 \chi_1^T &= \uparrow\uparrow\uparrow\uparrow, \\
 \chi_2^T &= \frac{1}{2}(\uparrow\uparrow\uparrow\downarrow + \uparrow\uparrow\downarrow\uparrow - \uparrow\downarrow\uparrow\uparrow - \downarrow\uparrow\uparrow\uparrow), \\
 \chi_3^T &= \frac{1}{\sqrt{3}}(\uparrow\uparrow\downarrow\downarrow + \downarrow\downarrow\uparrow\uparrow), \\
 &\quad - \frac{1}{2\sqrt{3}}(\uparrow\downarrow\uparrow\downarrow + \uparrow\downarrow\downarrow\uparrow + \downarrow\uparrow\uparrow\downarrow + \downarrow\uparrow\downarrow\uparrow) \\
 \chi_4^T &= \frac{1}{\sqrt{2}}(\uparrow\uparrow\uparrow\downarrow - \uparrow\uparrow\downarrow\uparrow), \\
 \chi_5^T &= \frac{1}{\sqrt{2}}(\uparrow\downarrow\uparrow\uparrow - \downarrow\uparrow\uparrow\uparrow), \\
 \chi_6^T &= \frac{1}{2}(\uparrow\downarrow\uparrow\downarrow - \uparrow\downarrow\downarrow\uparrow - \downarrow\uparrow\uparrow\downarrow + \downarrow\uparrow\downarrow\uparrow),
 \end{aligned} \tag{14}$$

where the notation uparrow stands for the state of spin upward, and the downarrow for the state of spin downwards. Given the spin wavefunctions (14), one can then compute the spin matrices $\langle \sigma_i \cdot \sigma_j \rangle$ of tetraquark states via the formulas (B2) in Appendix B. There are six spin matrices for the tetraquark in the subspace of $\{\chi_{1-6}^T\}$, which are

$$\langle \sigma_1 \cdot \sigma_2 \rangle = \begin{bmatrix} 1 & 0 & 0 & 0 & 0 & 0 \\ 0 & 1 & 0 & 0 & 0 & 0 \\ 0 & 0 & 1 & 0 & 0 & 0 \\ 0 & 0 & 0 & 1 & 0 & 0 \\ 0 & 0 & 0 & 0 & -3 & 0 \\ 0 & 0 & 0 & 0 & 0 & -3 \end{bmatrix}, \tag{15}$$

$$\langle \sigma_1 \cdot \sigma_3 \rangle = \begin{bmatrix} 1 & 0 & 0 & 0 & 0 & 0 \\ 0 & -1 & 0 & \sqrt{2} & -\sqrt{2} & 0 \\ 0 & 0 & -2 & 0 & 0 & -\sqrt{3} \\ 0 & \sqrt{2} & 0 & 0 & 1 & 0 \\ 0 & -\sqrt{2} & 0 & 1 & 0 & 0 \\ 0 & 0 & -\sqrt{3} & 0 & 0 & 0 \end{bmatrix}, \tag{16}$$

$$\langle \sigma_1 \cdot \sigma_4 \rangle = \begin{bmatrix} 1 & 0 & 0 & 0 & 0 & 0 \\ 0 & -1 & 0 & -\sqrt{2} & -\sqrt{2} & 0 \\ 0 & 0 & -2 & 0 & 0 & \sqrt{3} \\ 0 & -\sqrt{2} & 0 & 0 & -1 & 0 \\ 0 & -\sqrt{2} & 0 & -1 & 0 & 0 \\ 0 & 0 & \sqrt{3} & 0 & 0 & 0 \end{bmatrix}, \tag{17}$$

$$\langle \sigma_2 \cdot \sigma_3 \rangle = \begin{bmatrix} 1 & 0 & 0 & 0 & 0 & 0 \\ 0 & -1 & 0 & \sqrt{2} & \sqrt{2} & 0 \\ 0 & 0 & -2 & 0 & 0 & \sqrt{3} \\ 0 & \sqrt{2} & 0 & 0 & -1 & 0 \\ 0 & \sqrt{2} & 0 & -1 & 0 & 0 \\ 0 & 0 & \sqrt{3} & 0 & 0 & 0 \end{bmatrix}, \tag{18}$$

$$\langle \sigma_2 \cdot \sigma_4 \rangle = \begin{bmatrix} 1 & 0 & 0 & 0 & 0 & 0 \\ 0 & -1 & 0 & -\sqrt{2} & \sqrt{2} & 0 \\ 0 & 0 & -2 & 0 & 0 & -\sqrt{3} \\ 0 & -\sqrt{2} & 0 & 0 & 1 & 0 \\ 0 & \sqrt{2} & 0 & 1 & 0 & 0 \\ 0 & 0 & -\sqrt{3} & 0 & 0 & 0 \end{bmatrix}, \tag{19}$$

$$\langle \sigma_3 \cdot \sigma_4 \rangle = \begin{bmatrix} 1 & 0 & 0 & 0 & 0 & 0 \\ 0 & 1 & 0 & 0 & 0 & 0 \\ 0 & 0 & 1 & 0 & 0 & 0 \\ 0 & 0 & 0 & -3 & 0 & 0 \\ 0 & 0 & 0 & 0 & 1 & 0 \\ 0 & 0 & 0 & 0 & 0 & -3 \end{bmatrix} \tag{20}$$

2.3 Properties of triply heavy tetraquark states

In the framework of MIT bag model, the masses magnetic moment and charge radii can all be calculated for the ground state hadrons, as shown in Sect. 2.1. Given the model parameters and formulas in Sect. 2, one can then compute the masses of the triply heavy tetraquark states. We review in this subsection the related relations for other properties (magnetic moments and charge radii) of triply heavy tetraquark states.

Following the method in bag model [47], the contribution of a quark i or an antiquark i with electric charge Q_i to the charge radii of hadron is

$$\begin{aligned} \langle r_E^2 \rangle_i &= Q_i R^2 \frac{\alpha_i [2x_i^2 (\alpha_i - 1) + 4\alpha_i + 2\lambda_i - 3]}{3x_i^2 [2\alpha_i (\alpha_i - 1) + \lambda_i]} \\ &- Q_i R^2 \frac{\lambda_i [4\alpha_i + 2\lambda_i - 2x_i^2 - 3]}{2x_i^2 [2\alpha_i (\alpha_i - 1) + \lambda_i]}. \end{aligned} \tag{21}$$

Summing all of these contributions in Eq. (21) gives rise to the charge radii of hadron [47],

$$r_E = \left| \sum_i \langle r_E^2 \rangle_i \right|^{1/2}. \tag{22}$$

Note that Eq. (22) also holds true when the system has the identical quark constituents so that chromomagnetic interaction may yield spin-color state mixing.

Table 1 Sum rule for magnetic moments of tetraquarks ($q_1 q_2$) ($\bar{q}_3 \bar{q}_4$) and their spin-mixed systems

ψ_{spin}	μ
χ_1^T	$\mu_1 + \mu_2 + \mu_3 + \mu_4$
χ_2^T	$\frac{1}{2} (\mu_1 + \mu_2 + \mu_3 + \mu_4)$
χ_3^T	0
χ_4^T	$\mu_1 + \mu_2$
χ_5^T	$\mu_3 + \mu_4$
χ_6^T	0
$C_1 \chi_3^T + C_2 \chi_6^T$	0

For the magnetic moment, the related formula is [45,47].

$$\mu_i = Q_i \bar{\mu}_i = Q_i \frac{R}{6} \frac{4\omega_i R + 2m_i R - 3}{2\omega_i R (\omega_i R - 1) + m_i R}, \tag{23}$$

$$\mu = \langle \psi_{spin} \left| \sum_i g_i \mu_i S_{iz} \right| \psi_{spin} \rangle, \tag{24}$$

where $g_i = 2$ and S_{iz} is the third component of quark i and antiquark i .

We list in the Table 1 all magnetic moment formulas as a sum rule for the triply heavy tetraquarks. Given spin wavefunction χ_{1-6}^T , the corresponding magnetic moment of triply heavy tetraquark states can be calculated via Table 1. In the case of spin mixing, the computation goes in the following way: The spin wavefunction $C_1 \chi_2^T + C_2 \chi_4^T + C_3 \chi_5^T$ contributes to magnetic moment by $C_1^2 \mu (\chi_2^T) + C_2^2 \mu (\chi_4^T) + C_3^2 \mu (\chi_5^T) + \sqrt{2} C_1 C_2 (\mu_3 - \mu_4) + \sqrt{2} C_1 C_3 (\mu_2 - \mu_1)$, the spin wave function $C_1 \chi_2^T + C_2 \chi_5^T + C_3 \chi_4^T$ contributes $C_1^2 \mu (\chi_2^T) + C_2^2 \mu (\chi_5^T) + C_3^2 \mu (\chi_4^T) + \sqrt{2} C_1 C_2 (\mu_2 - \mu_1) + \sqrt{2} C_1 C_3 (\mu_3 - \mu_4)$.

In addition, we present the way to compute the decay width Γ_I of the tetraquark state [46], which is given by

$$\Gamma_I = \gamma_I \alpha \frac{p^{2L+1}}{m^{2L}} \cdot |c_I|^2, \tag{25}$$

with γ_I the prefactor involving decay dynamics, α a coupling constant at decay vertex, p is the momentum of final hadrons (two mesons M_1 and M_2), m the mass of initial tetraquark state and c_I eigenvector of the I -th decay channel. The factor γ_I varies depending upon the initial tetraquark and the final decay state and it differs for each decay channel. Notice that the following prefactors are nearly same

$$\gamma_{M_1 M_2} = \gamma_{M_1^* M_2} = \gamma_{M_1 M_2^*} = \gamma_{M_1^* M_2^*} \tag{26}$$

for the final channel $M_1 M_2$, $M_1^* M_2$, $M_1 M_2^*$ and $M_1^* M_2^*$ where $M_{1,2}$ and $M_{1,2}^*$ stand for the mesons or excited mesons in the final decay states, respectively.

3 Numerical results

Given the model parameters and formulas detailed in Sect. 2, one can compute the masses, magnetic moments and charge radii of all ground (strange and nonstrange) states of triply heavy tetraquarks. For this purpose, we proceed this computation for the tetraquarks with three heavy quarks(antiquarks) by grouping them into four classes, namely, the triply heavy tetraquarks $nb\bar{Q}\bar{Q}$ and $nc\bar{Q}\bar{Q}$, the triply heavy tetraquarks $sc\bar{Q}\bar{Q}$, $sb\bar{Q}\bar{Q}$, the triply heavy tetraquarks $nQ\bar{Q}\bar{Q}'$ and the triply heavy tetraquarks $sQ\bar{Q}\bar{Q}'$, as to be addressed in the following subsections. We use the notation $T(qQ''\bar{Q}\bar{Q}', M, J^P)$ denote the triply heavy tetraquark with flavor content $qQ''\bar{Q}\bar{Q}'$, mass M in GeV and the spin-parity J^P , for simplicity.

3.1 Triply heavy tetraquarks $nb\bar{Q}\bar{Q}$ and $nc\bar{Q}\bar{Q}$.

We consider first the triply heavy tetraquarks $nb\bar{Q}\bar{Q}$ and $nc\bar{Q}\bar{Q}$ ($Q = c, b$) with identical flavor of two heavy antiquark. Owing to the chromomagnetic interaction (3), the color-spin states ($\phi\chi$) of tetraquark $nb\bar{Q}\bar{Q}$ or $nc\bar{Q}\bar{Q}$ can mix among them to form a mixed state, a linear superposition of spin-color bases. For the heavy tetraquark, the $J^P = 2^+$ state consists of one state ($\phi_2\chi_1$), with no mixing. The $J^P = 1^+$ state consists of three basis states ($\phi_2\chi_2, \phi_2\chi_5, \phi_1\chi_4$) and can mix into a mixed state having the form of $c_1\phi_2\chi_2 + c_2\phi_2\chi_5 + c_3\phi_1\chi_4$. Meanwhile, the $J^P = 0^+$ state, consisting of two basis states ($\phi_2\chi_3, \phi_1\chi_6$), can mix into the mixed states with the form $c_1\phi_2\chi_3 + c_2\phi_1\chi_6$.

First of all, we write the mass formula for the triply heavy tetraquarks $nb\bar{Q}\bar{Q}$ and $nc\bar{Q}\bar{Q}$ with $J^P = 2^+, 1^+, 0^+$, which are obtained via diagonalization of the CMI for $J^P = 1^+$ and 0^+ multiplets(mixed states). Then, one can minimize the diagonalized mass (1) using the variational method to find the respective optimal bag radii R of the tetraquark and to solve x_i depending on R via the transcendental equation(A3) interactively. This leads to the tetraquark masses (1) for each of the triply heavy tetraquark states, as shown in Figs. 1 and 2. Further, one can use Eqs. (22) and (24) to compute their charge radii and magnetic moments, and use Eq. (25) to estimate the relative decay widths of the tetraquark for the two-meson channel depicted in Fig. 1.

In Table 2, we list the obtained mass(in GeV), magnetic moments(in μ_N) and charge radii (in fm) of the triply heavy tetraquarks $nb\bar{Q}\bar{Q}$ and $nc\bar{Q}\bar{Q}$, which contain four states with given J^P : $nb\bar{b}\bar{b}$, $nb\bar{c}\bar{c}$, $nc\bar{b}\bar{b}$, and $nc\bar{c}\bar{c}$. For the tetraquark $nb\bar{b}\bar{b}$, the $J^P = 0^+$ state has mass of 15.335 GeV for the mixed configuration dominated relatively by $\bar{3}_c \otimes 3_c$ and has the mass of 15.401 GeV for the mixed configuration dominated relatively by $6_c \otimes \bar{6}_c$. The later (in $6_c \otimes \bar{6}_c$) are heavier than the former(in $\bar{3}_c \otimes 3_c$) about 0.066 GeV. As depicted in Fig. 1, this state may decay to the final two-meson states

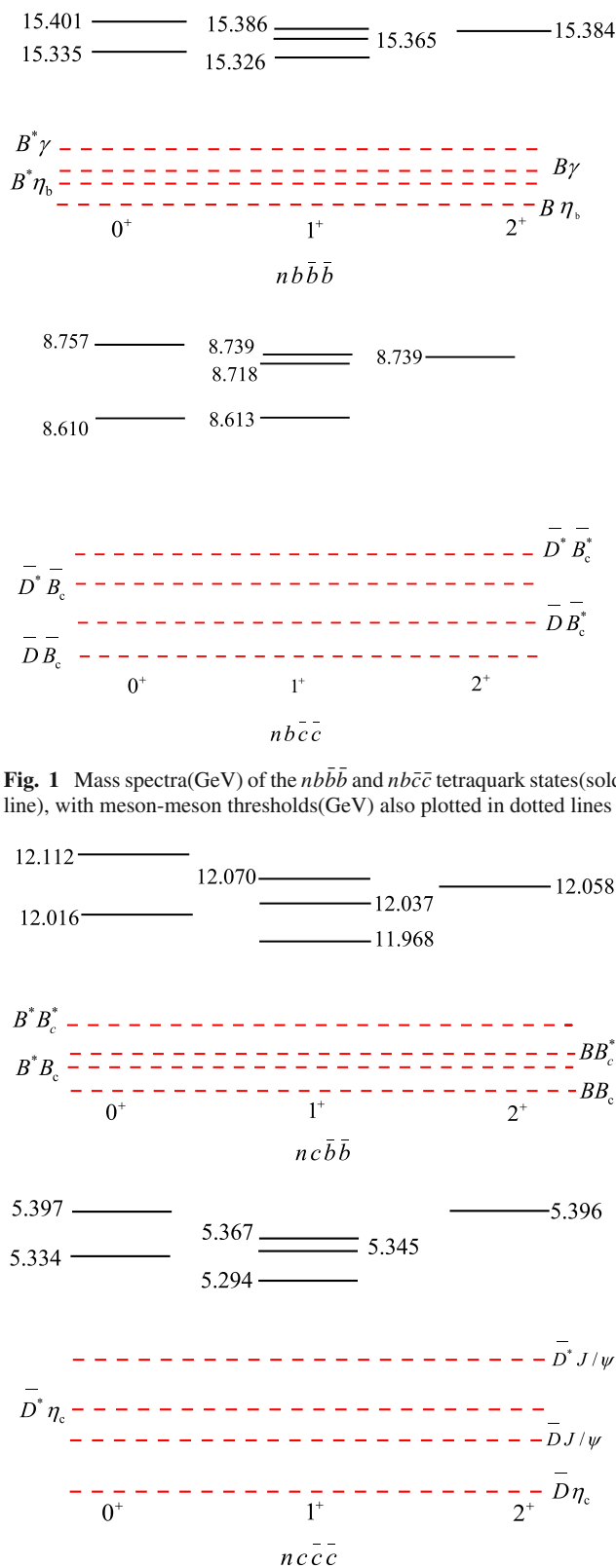


Fig. 1 Mass spectra(GeV) of the $nb\bar{b}\bar{b}$ and $nb\bar{c}\bar{c}$ tetraquark states(solid line), with meson-meson thresholds(GeV) also plotted in dotted lines

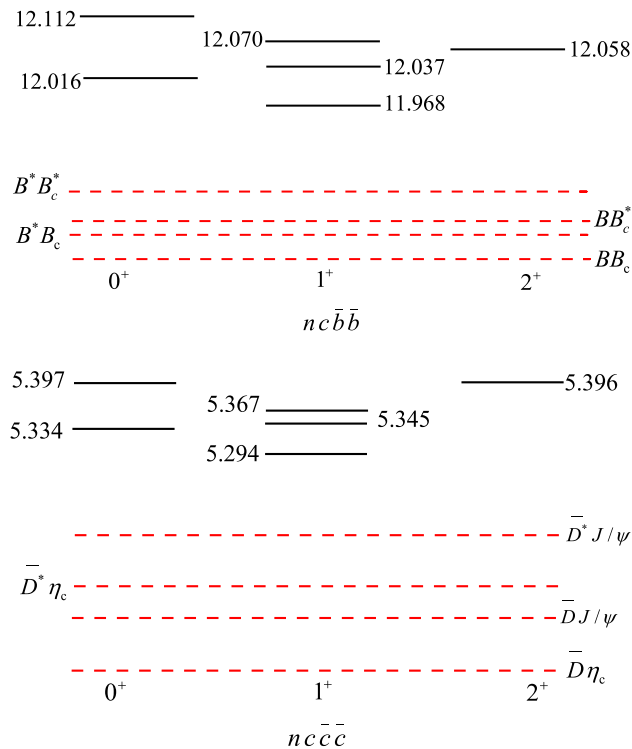


Fig. 2 Mass spectra(GeV) of the $nc\bar{b}\bar{b}$ and $nc\bar{c}\bar{c}$ tetraquark states in solid line, with meson-meson thresholds (GeV) plotted in dotted lines

Table 2 Computed masses (in GeV), magnetic moments(in μ_N) and charge radii (in fm) of triply heavy tetraquarks $nb\bar{Q}\bar{Q}$. Bag radii R_0 is in GeV^{-1} . The first and second values charge radii (magnetic moment) correspond to $n=u$ and $n=d$, respectively

State	J^P	Eigenvector	R_0	M_{bag}	r_E (fm)	μ_{bag}	[46]
$(nb\bar{b}\bar{b})$	2^+	1.00	4.14	15.384	0.55, 0.23	1.56, -0.65	14.872
	1^+	(-0.65, -0.19, 0.74)	4.12	15.386	0.55, 0.23	0.82, -0.47	14.852
		(0.64, -0.67, 0.39)	4.07	15.365	0.54, 0.22	1.52, -0.56	14.852
		(0.42, 0.72, 0.55)	3.96	15.326	0.53, 0.22	-0.02, 0.06	14.712
		(0.58, 0.81)	4.19	15.401	0.56, 0.23	-	14.706
	0^+	(-0.81, 0.58)	3.99	15.335	0.53, 0.22	-	14.851
$(nb\bar{c}\bar{c})$	2^+	1.00	4.77	8.739	0.40, 0.79	0.63, -1.92	8.478
	1^+	(-0.63, -0.35, 0.70)	4.74	8.739	0.40, 0.80	0.23, -0.71	8.454
		(0.60, -0.79, 0.13)	4.67	8.718	0.39, 0.78	0.70, -1.47	8.430
		(0.50, 0.50, 0.70)	4.52	8.613	0.38, 0.75	-0.05, -0.66	8.218
		(0.69, 0.73)	4.84	8.757	0.81, 0.81	-	8.445
	0^+	(-0.73, 0.68)	4.54	8.610	0.76, 0.76	-	8.199
$(nc\bar{b}\bar{b})$	2^+	1.00	4.50	12.058	0.78, 0.44	2.26, -0.14	11.652
	1^+	(-0.36, -0.17, 0.92)	4.40	12.070	0.76, 0.43	1.80, -0.15	11.659
		(0.93, -0.19, 0.33)	4.40	12.037	0.76, 0.43	1.45, -0.40	11.625
		(0.12, 0.97, 0.23)	4.25	11.968	0.74, 0.41	0.11, 0.35	11.582
		(0.38, 0.93)	4.55	12.112	0.79, 0.44	-	11.695
	0^+	(-0.92, 0.38)	4.36	12.016	0.76, 0.42	-	11.582
$(nc\bar{c}\bar{c})$	2^+	1.00	5.01	5.396	0.37, 0.62	1.29, -1.39	5.198
	1^+	(-0.87, -0.05, 0.49)	4.88	5.367	0.36, 0.61	0.92, -0.52	5.154
		(0.47, -0.37, 0.80)	4.86	5.345	0.35, 0.60	0.92, -0.52	5.136
		(0.14, 0.93, 0.35)	4.76	5.294	0.35, 0.59	0.89, -0.51	4.968
		(0.36, 0.83)	5.01	5.397	0.37, 0.62	-	4.937
	0^+	(-0.83, 0.55)	4.87	5.334	0.36, 0.60	-	5.185

Table 3 Computed masses(in GeV), magnetic moments and charge radii of triply heavy tetraquarks $sb\bar{Q}\bar{Q}$ and $sc\bar{Q}\bar{Q}$. Bag radii R_0 is in GeV^{-1}

State	J^P	Eigenvector	R_0	M_{bag}	r_E (fm)	μ_{bag}	[46]
$(sb\bar{b}\bar{b})$	2^+	1.00	4.22	15.476	0.19	-0.52	14.957
	1^+	(-0.63, -0.21, 0.75)	4.07	15.476	0.19	-0.38	14.944
		(0.66, -0.66, 0.37)	4.02	15.458	0.19	-0.43	14.929
		(0.41, 0.73, 0.55)	3.91	15.424	0.18	-0.06	14.805
		(0.58, 0.81)	4.26	15.492	0.20	-	14.936
	0^+	(-0.81, 0.58)	4.09	15.433	0.19	-	14.793
$(sb\bar{c}\bar{c})$	2^+	1.00	4.82	8.840	0.79	-1.74	8.569
	1^+	(-0.83, -0.07, 0.55)	4.65	8.823	0.76	-0.78	8.553
		(0.52, -0.48, 0.71)	4.64	8.794	0.76	-0.77	8.522
		(0.22, 0.87, 0.44)	4.53	8.736	0.74	-0.77	8.325
		(0.73, 0.68)	4.84	8.839	0.79	-	8.301
	0^+	(-0.69, 0.72)	4.70	8.783	0.77	-	8.539
$(sc\bar{b}\bar{b})$	2^+	1.00	4.55	12.158	0.46	2.26	11.652
	1^+	(-0.37, -0.19, 0.91)	4.36	12.162	0.44	0.01	11.659

Table 3 continued

State	J^P	Eigenvector	R_0	M_{bag}	r_E (fm)	μ_{bag}	[46]
$(sc\bar{c}\bar{c})$	0^+	(0.92, -0.19, 0.34)	4.35	12.138	0.44	-0.27	11.625
		(0.11, 0.96, 0.25)	4.21	12.078	0.43	0.35	11.582
		(0.40, 0.91)	4.60	12.200	0.47	-	11.582
		(-0.91, 0.41)	4.43	12.119	0.45	-	11.695
	2^+	1.00	5.05	5.504	0.60	-1.19	5.303
		(-0.43, 0.40, 0.81)	4.90	5.499	0.59	-0.10	5.254
	1^+	(0.85, -0.49, 0.20)	4.83	5.464	0.58	-1.35	5.240
		(0.31, 0.77, 0.55)	4.68	5.391	0.56	-0.30	5.069
		(0.58, 0.81)	5.13	5.540	0.61	-	5.040
		(-0.81, 0.58)	4.80	5.391	0.58	-	5.291

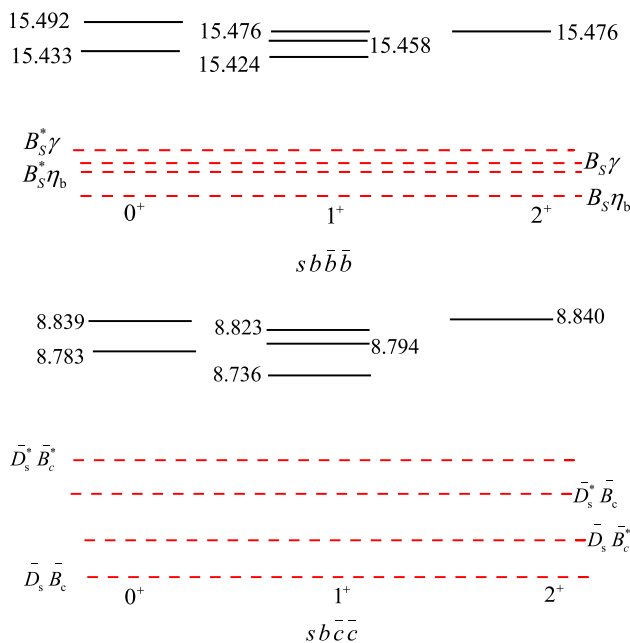


Fig. 3 Mass spectra(GeV) of the tetraquarks $sb\bar{b}\bar{b}$ and $sb\bar{c}\bar{c}$ plotted in solid line. The meson-meson thresholds (GeV) are also shown in dotted lines

of the $B^*\Upsilon$, $B\Upsilon$, $B^*\eta_b$ or $B\eta_b$. Our computation via Eq. (25) shows that the tetraquark $T(nb\bar{b}\bar{b}, 15.401, J^P = 0^+)$ can predominantly decay to $B^*\Upsilon$, with the relative decay widths of $\Gamma_{B^*\Upsilon} : \Gamma_{B\eta_b} \sim 1.15 : 0.004$. In addition, it turns out that tetraquark $T(nb\bar{b}\bar{b}, 15.386, J^P = 1^+)$ can predominantly decay into $B^*\Upsilon$ or $B^*\eta_b$, with relative decay widths of $\Gamma_{B^*\Upsilon} : \Gamma_{B^*\eta_b} : \Gamma_{B\Upsilon} \sim 0.52 : 0.56 : 0.001$.

For the tetraquark state $nb\bar{c}\bar{c}$, the $J^P = 0^+$ state has mass of 8.757 GeV in the mixed state with configuration $6_c \otimes \bar{6}_c$. dominated relatively and has mass of 8.610 GeV with $\bar{3}_c \otimes 3_c$ dominated relatively, with the later lighter than the former about 0.147 GeV. As indicated in Fig. 1, this state may decay to $\bar{D}^*\bar{B}_c^*$, $\bar{D}^*\bar{B}_c$, $\bar{D}\bar{B}_c^*$ or $\bar{D}\bar{B}_c$. The tetraquark $T(nb\bar{c}\bar{c}, 8.757, J^P = 0^+)$ can decay dominantly to the chan-

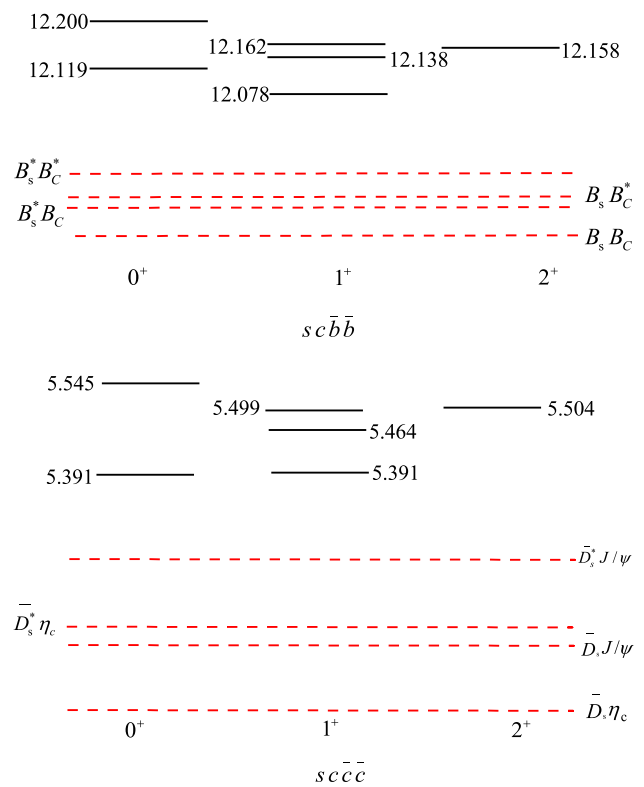


Fig. 4 Mass spectra(GeV) of the tetraquarks $sc\bar{b}\bar{b}$ and $sc\bar{c}\bar{c}$ plotted in solid line. The meson-meson thresholds (GeV) are shown in dotted lines

nel $\bar{D}^*\bar{B}_c^*$, while the tetraquark $T(nb\bar{c}\bar{c}, 8.739, J^P = 1^+)$ can predominantly decay to $\bar{D}^*\bar{B}_c^*$ or $\bar{D}^*\bar{B}_c$. The relative widths of them are $\Gamma_{\bar{D}^*\bar{B}_c^*} : \Gamma_{\bar{D}^*\bar{B}_c} \sim 0.59 : 0.003$ and $\Gamma_{\bar{D}^*\bar{B}_c^*} : \Gamma_{\bar{D}^*\bar{B}_c} : \Gamma_{\bar{D}\bar{B}_c^*} \sim 0.34 : 0.27 : 0.006$.

For the tetraquark $nc\bar{b}\bar{b}$, the $J^P = 0^+$ state has mass of 12.016 GeV in the mixed state with configuration $\bar{3}_c \otimes 3_c$ dominated relatively and has mass of 12.112 GeV with $6_c \otimes \bar{6}_c$. dominated relatively, with the later heavier than the former about 0.096 GeV. As shown in Fig. 2, this state may

Table 4 Computed masses (in GeV) triply heavy tetraquarks $nQ\bar{Q}\bar{Q}'$, with bag radii R_0 in GeV^{-1} . The masses are compared to other calculations cited. The charge radii are 0.32 fm (n=u) or 0.55 fm (n=d) for the tetraquark $nb\bar{c}\bar{b}$; They are 0.62 fm (n=u) or 0.26 fm (n=d) for the

$nc\bar{c}\bar{b}$. The Bag radii R_0 are 4.430 GeV^{-1} for $nb\bar{c}\bar{b}$ and 4.700 GeV^{-1} for $nc\bar{c}\bar{b}$. The first and second values magnetic moment correspond to n=u and n=d, respectively

State	J^P	Eigenvector	M_{bag}	μ_{bag}	[46]	Scattering state
$(nb\bar{c}\bar{b})$	2^+	1.00	11.927	1.09, -1.28	11.545	$\bar{D}^*\Upsilon$
		1.00	12.067	1.09, -1.28	11.748	
	1^+	(-0.15, 0.17, -0.14, 0.77, -0.37, 0.44)	11.809	0.63, -0.34	11.315	$\bar{D}\Upsilon$
		(-0.16, -0.11, -0.17, -0.34, -0.88, -0.22)	11.897	-0.02, -1.00	11.392	
		(-0.10, 0.08, 0.8, -0.52, -0.02, 0.84)	11.924	-0.01, -0.59	11.447	
		(0.41, -0.21, 0.83, 0.11, -0.27, 0.06)	12.029	0.98, -0.74	11.698	
		(-0.63, 0.57, 0.48, -0.04, 0.017, -0.20)	12.049	2.00, -0.70	11.719	
	0^+	(0.61, 0.76, -0.13, -0.11, -0.12, -0.05)	12.056	-0.28, -0.47	11.745	$\bar{D}\eta_b$ $B^*\bar{B}_c^*$
		(-0.16, -0.23, 0.93, 0.26)	11.797	-	11.253	
		(-0.32, 0.10, -0.28, 0.90)	11.898	-	11.439	
$(nc\bar{c}\bar{b})$	2^+	(0.26, 0.93, 0.26, 0.07)	12.027	-	11.673	$\bar{D}^*\bar{B}_c^*$
		(0.90, -0.28, -0.013, 0.35)	12.046	-	11.749	
	1^+	1.00	8.727	1.76, -0.75	8.335	$\bar{D}^*\bar{B}_c^*$
		1.00	8.747	1.76, -0.75	8.469	
		(0.27, -0.23, 0.60, -0.56, 0.39, -0.23)	8.596	0.18, -0.14	8.190	
		(-0.14, 0.43, 0.69, 0.42, 0.11, 0.35)	8.658	-0.11, -0.41	8.268	
		(-0.79, 0.09, 0.06, -0.55, -0.20, 0.17)	8.693	1.22, -0.54	8.313	
	0^+	(-0.20, -0.69, 0.36, 0.33, -0.47, -0.19)	8.709	3.26, -0.64	8.399	$\bar{D}\bar{B}_c$
		(0.45, 0.33, 0.17, -0.29, -0.76, 0.04)	8.739	0.59, -0.17	8.436	
		(0.22, -0.42, -0.07, -0.13, 0.03, 0.87)	8.765	0.15, -0.35	8.457	
(0.20, 0.63, -0.74, -0.13)		8.566	-	8.123		
(0.80, -0.34, 0.01, -0.50)		8.649	-	8.281		
	(0.24, 0.70, 0.67, -0.07)	8.691	-	8.388		
	(0.52, -0.04, -0.05, 0.85)	8.779	-	8.466		

decay to $B^*B_c^*$, BB_c^* , B^*B_c or BB_c . The dominant decay channel of the tetraquark $T(nc\bar{b}\bar{b}, 12.112, J^P = 0^+)$ is $B^*B_c^*$, while the tetraquark $T(nc\bar{b}\bar{b}, 12.070, J^P = 1^+)$ can predominantly decay to $B^*B_c^*$ or B^*B_c . The relative decay widths $\Gamma_{B^*B_c^*} : \Gamma_{BB_c} \sim 0.95 : 0.063$ and $\Gamma_{B^*B_c^*} : \Gamma_{B^*B_c} : \Gamma_{BB_c} \sim 0.56 : 0.37 : 0.06$.

For the tetraquark $nc\bar{c}\bar{c}$, the $J^P = 0^+$ state has mass of 5.334 GeV in the mixed state with configuration $\bar{3}_c \otimes 3_c$ dominated relatively and has mass of 5.397 GeV with $6_c \otimes \bar{6}_c$ dominated relatively, with the later heavier than the former about 0.063 GeV. As depicted in Fig. 2, the 0^+ state can decay to \bar{D}^*J/ψ , $\bar{D}^*\eta_c$, $\bar{D}J/\psi$ or $\bar{D}\eta_c$. The dominant channel of the tetraquark $T(nc\bar{c}\bar{c}, 5.397, J^P = 0^+)$ is the \bar{D}^*J/ψ , while the tetraquark $T(nc\bar{c}\bar{c}, 5.367, J^P = 1^+)$ can predominantly decay to \bar{D}^*J/ψ or $\bar{D}^*\eta_c$, with the relative width $\Gamma_{\bar{D}^*J/\psi} : \Gamma_{\bar{D}\eta_c} \sim 0.36 : 0.04$. The decay width ratio is $\Gamma_{\bar{D}^*J/\psi} : \Gamma_{\bar{D}^*\eta_c} : \Gamma_{\bar{D}J/\psi} \sim 0.12 : 0.14 : 0.07$.

In Table 2, we also compare our calculated tetraquark masses to that in Ref. [46], with mass difference about 0.2 – 0.5 GeV.

3.2 Triply heavy tetraquarks $sb\bar{Q}\bar{Q}$ and $sc\bar{Q}\bar{Q}$

Due to chromomagnetic interaction, the triply heavy tetraquarks $sb\bar{Q}\bar{Q}$ and $sc\bar{Q}\bar{Q}$ can mix their spin-color bases to form mixed states, a linear combination of spin-color basis functions ($\phi\chi$). A $J^P = 2^+$ state of tetraquark consists of a singlet $\phi_2\chi_1$ while the $J^P = 1^+$ state consist of the mixed states $c_1\phi_2\chi_2 + c_2\phi_2\chi_5 + c_3\phi_1\chi_4$ in the subspace ($\phi_2\chi_2, \phi_2\chi_5, \phi_1\chi_4$); the $J^P = 0^+$ state is composed of the mixed state $c_1\phi_2\chi_3 + c_2\phi_1\chi_6$ in the subspace ($\phi_2\chi_3, c_2\phi_1\chi_6$). Similarly, we employ MIT bag mode to compute the masses, bag radii, magnetic moments, and charge radii of the triply heavy tetraquarks $sb\bar{Q}\bar{Q}$ and $sc\bar{Q}\bar{Q}$ with the spin-color wavefunctions. The results are shown in Table 3.

The triply heavy tetraquarks $sb\bar{Q}\bar{Q}$ and $sc\bar{Q}\bar{Q}$ consist in flavor context of the four states: the tetraquark $sb\bar{b}\bar{b}$, the $sb\bar{c}\bar{c}$, the $sc\bar{b}\bar{b}$, and the $sc\bar{c}\bar{c}$. In the case of the $sb\bar{b}\bar{b}$, the $J^P = 0^+$ state has mass of 15.433 GeV in the mixed state with configuration $\bar{3}_c \otimes 3_c$ dominated relatively and has mass of 15.492 GeV with $6_c \otimes \bar{6}_c$ dominated relatively, with the

later heavier than the former about 0.059 GeV. This state can decay into the final two-meson states of the $B_s^* \Upsilon$, $B_s \Upsilon$, $B_s^* \eta_b$ or $B_s \eta_b$, as shown in Fig. 3. We find that relative decay width between the channels $B_s^* \Upsilon$ and $B_s \eta_b$ is $\Gamma_{B_s^* \Upsilon} : \Gamma_{B_s \eta_b} \sim 0.07 : 0.94$. The state $T(sbb\bar{b}, 15.492, 0^+)$ can dominantly decay into $B_s \eta_b$ whereas the state $T(sbb\bar{b}, 15.476, 1^+)$ can primarily decay into $B_s^* \Upsilon$ or $B_s^* \eta_b$, with computed relative decay width $\Gamma_{B_s^* \Upsilon} : \Gamma_{B_s^* \eta_b} : \Gamma_{B_s \Upsilon} \sim 0.53 : 0.55 : 0.001$.

Regarding the tetraquark $sb\bar{c}\bar{c}$, $J^P = 0^+$ state has mass of 8.783 GeV in the mixed state with configuration $6_c \otimes \bar{6}_c$ dominated relatively and has mass of 8.839 GeV with $\bar{3}_c \otimes 3_c$ dominated relatively, with the later heavier than the former about 0.056 GeV. As illustrated in Fig. 3, the tetraquark $sb\bar{c}\bar{c}$ can potentially decay to $\bar{D}_s^* \bar{B}_c^*$, $\bar{D}_s^* \bar{B}_c$, $\bar{D}_s \bar{B}_c^*$ or $\bar{D}_s \bar{B}_c$, with the relative decay widths about $\Gamma_{\bar{D}_s^* \bar{B}_c^*} : \Gamma_{\bar{D}_s \bar{B}_c} \sim 0.59 : 0.001$. The tetraquark $T(sb\bar{c}\bar{c}, 8.839, 0^+)$ can decay into $\bar{D}_s^* \bar{B}_c^*$ dominantly, while $T(sb\bar{c}\bar{c}, 8.823, 1^+)$ can primarily decay into $\bar{D}_s^* \bar{B}_c^*$ or $\bar{D}_s^* \bar{B}_c$, with relative decay width of $\Gamma_{\bar{D}_s^* \bar{B}_c^*} : \Gamma_{\bar{D}_s \bar{B}_c} : \Gamma_{\bar{D}_s \bar{B}_c^*} \sim 0.14 : 0.24 : 0.009$.

For the tetraquark $sc\bar{b}\bar{b}$, the 0^+ state has the mass of 12.119 GeV for the dominated rep. $\bar{3}_c \otimes 3_c$ configuration and the mass of 12.200 GeV for the dominated rep $6_c \otimes \bar{6}_c$ (heavier than the former about 0.081 GeV). As shown in Fig. 4, the decay channels of this state contain potentially $B_s^* B_c^*$, $B_s B_c^*$, $B_s^* B_c$, and $B_s B_c$. The state $T(sc\bar{b}\bar{b}, 12.200, 0^+)$ can decay to $B_s^* B_c^*$, whereas $T(sc\bar{b}\bar{b}, 12.162, J^P = 1^+)$ to $B_s^* B_c^*$ or $B_s^* B_c$, with computed relative decay widths $\Gamma_{B_s^* B_c^*} : \Gamma_{B_s B_c} \sim 0.95 : 0.05$ and $\Gamma_{B_s^* B_c^*} : \Gamma_{B_s^* B_c} : \Gamma_{B_s B_c} \sim 0.57 : 0.37 : 0.05$.

In the case of the tetraquark $sc\bar{c}\bar{c}$, the 0^+ state has the mass of 5.391 GeV for the dominated rep. $\bar{3}_c \otimes 3_c$ configuration and the mass of 5.545 GeV for the dominated rep. $6_c \otimes \bar{6}_c$ (heavier than the former 0.154 GeV). As depicted in Fig. 4, the potential decay channels of this state contain $\bar{D}_s^* J/\psi$, $\bar{D}_s^* \eta_c$, $\bar{D}_s J/\psi$, and $\bar{D}_s \eta_c$. The state $T(sc\bar{c}\bar{c}, 5.540, 0^+)$ can decay to $\bar{D}_s^* J/\psi$ dominantly, while the state $T(sc\bar{c}\bar{c}, 5.499, 1^+)$ can primarily decay to $\bar{D}_s^* J/\psi$ or $\bar{D}_s^* \eta_c$, with the relative decay width $\Gamma_{\bar{D}_s^* J/\psi} : \Gamma_{\bar{D}_s \eta_c} \sim 0.51 : 0.002$ and $\Gamma_{\bar{D}_s^* J/\psi} : \Gamma_{\bar{D}_s^* \eta_c} : \Gamma_{\bar{D}_s J/\psi} \sim 0.34 : 0.16 : 0.001$.

3.3 Triply heavy tetraquarks $nQ\bar{Q}\bar{Q}'$

This type of triply heavy tetraquarks consists of two classes of the tetraquark states: $nb\bar{c}\bar{b}$ and $nc\bar{c}\bar{b}$. The state with $J^P = 2^+$ contains two configurations ($\phi_2 \chi_1, \phi_1 \chi_1$) while the 1^+ state, spanned by the basis states ($\phi_2 \chi_2, \phi_2 \chi_4, \phi_2 \chi_5, \phi_1 \chi_2, \phi_1 \chi_4, \phi_1 \chi_5$), form a mixed state, $c_1 \phi_2 \chi_2 + c_2 \phi_2 \chi_4 + c_3 \phi_2 \chi_5 + c_4 \phi_1 \chi_2 + c_5 \phi_1 \chi_4 + c_6 \phi_1 \chi_5$. Additionally, the 0^+ state can be mixed state $c_1 \phi_2 \chi_3 + c_2 \phi_2 \chi_6 + c_3 \phi_1 \chi_3 + c_4 \phi_1 \chi_6$ in the space ($\phi_2 \chi_3, \phi_2 \chi_6, \phi_1 \chi_3, \phi_1 \chi_6$). Treating the CMI as perturbation, one can calculate the mass and other properties, as listed in Table 4. Given the computed masses (shown in Fig. 5) of the tetraquark $nc\bar{c}\bar{b}$, they exceed the thresh-

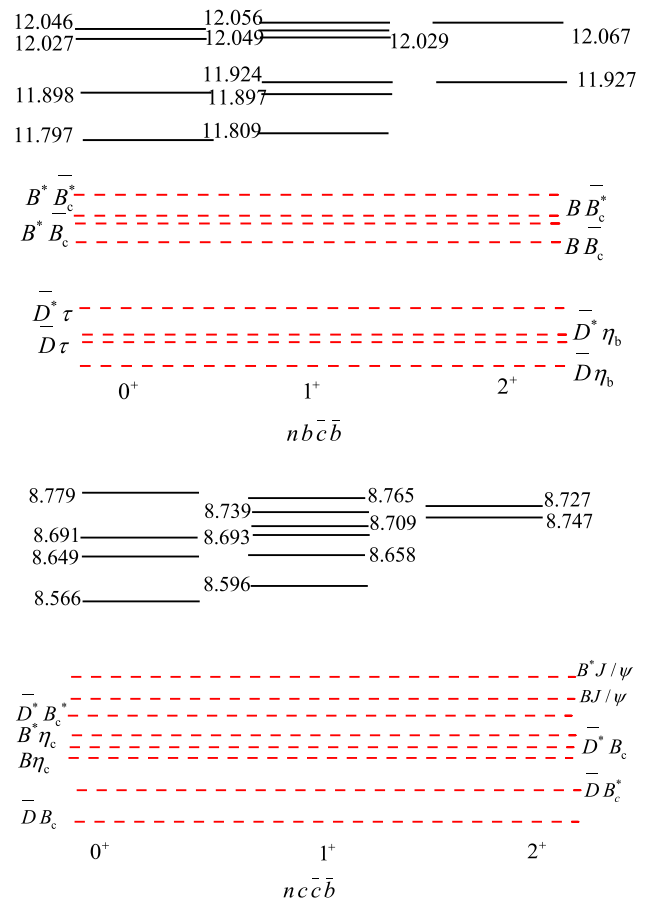


Fig. 5 Mass spectra(GeV, the solid lines) of the tetraquarks $nb\bar{c}\bar{b}$ and $nc\bar{c}\bar{b}$, with their two-meson thresholds(GeV) plotted as dotted lines

old and may decay to $B^* J/\psi$, $B J/\psi$, $\bar{D}^* \bar{B}_c^*$, $B^* \eta_c$, $\bar{D}^* \bar{B}_c$, $B \eta_c$, $\bar{D}^* \bar{B}_c^*$ or $\bar{D} \bar{B}_c$, as shown in Fig. 5. Notably, the analysis via eigenvector of the CMI matrix reveals that the state $T(nc\bar{c}\bar{b}, 8.747, 2^+)$ couples strongly to $\bar{D}^* \bar{B}_c^*$, while the $T(nc\bar{c}\bar{b}, 8.596, 1^+)$ couples significantly to $\bar{D}^* \bar{B}_c$. Furthermore, the state $T(nc\bar{c}\bar{b}, 8.566, 0^+)$ couples strongly to $\bar{D} \bar{B}_c$, a candidate of the scattering states.

Regarding the tetraquark $nb\bar{c}\bar{b}$, the main decay channels contain $B^* \bar{B}_c^*$, $B \bar{B}_c^*$, $B^* \bar{B}_c$, $B \bar{B}_c$, $\bar{D}^* \Upsilon$, $\bar{D}^* \eta_b$, $\bar{D} \Upsilon$ and $\bar{D} \eta_b$, as depicted in Fig. 5. Notably, analysis via computed masses and eigenvectors (shown in Table V), the state $T(nb\bar{c}\bar{b}, 11.927, 2^+)$ exhibit a pronounced coupling to $\bar{D}^* \Upsilon$, while the $T(nb\bar{c}\bar{b}, 11.809, 1^+)$ states display a strong coupling to $\bar{D} \Upsilon$. Additionally, the $T(nb\bar{c}\bar{b}, 11.898, 0^+)$ states demonstrate a robust coupling to $B^* \bar{B}_c^*$, whereas the state $T(nb\bar{c}\bar{b}, 11.797, 0^+)$ s exhibit a strong coupling to $\bar{D} \eta_b$, potentially indicating scattering states.

3.4 Triply heavy tetraquarks $sQ\bar{Q}\bar{Q}'$

The triply heavy tetraquarks $sQ\bar{Q}\bar{Q}'$ consists of two types of tetraquark states: the $sb\bar{c}\bar{b}$ and the $sc\bar{c}\bar{b}$. For them, the 2^+

Table 5 Computed masses (GeV) triply heavy tetraquarks $sQ\bar{Q}\bar{Q}'$, with bag radii R_0 in GeV^{-1} . The masses are compared to the other calculations. $(sb\bar{c}\bar{b})$ state's charge radii respectively are 0.54(fm); $(sb\bar{c}\bar{b})$

state's Bag radii R_0 respectively are 4.490 is in GeV^{-1} . $(sc\bar{c}\bar{b})$ state's charge radii respectively are 0.21(fm). $(sc\bar{c}\bar{b})$ state's Bag radii R_0 respectively are 4.75 is in GeV^{-1}

State	J^P	Eigenvector	M_{bag}	μ_{bag}	[46]	Scattering state
$(sb\bar{c}\bar{b})$	2^+	1.00	12.149	- 1.12	11.558	
		1.00	12.168	- 1.12	11.833	
	1^+	(- 0.29, 0.31, - 0.29, 0.66, - 0.37, - 0.40)	12.040	- 0.08	11.416	$\bar{D}_s \Upsilon$
		(- 0.33, - 0.35, - 0.52, - 0.34, - 0.55, - 0.29)	12.107	- 1.12	11.496	
		(- 0.57, 0.21, 0.41, - 0.50, - 0.10, 0.45)	12.134	- 0.95	11.549	
		(- 0.06, - 0.58, 0.62, 0.36, - 0.37, - 0.07)	12.151	- 0.81	11.785	
		(- 0.69, 0.01, 0.02, 0.26, 0.48, - 0.49)	12.166	- 0.35	11.803	
	0^+	(- 0.10, - 0.63, - 0.30, 0.03, 0.43, 0.56)	12.168	- 0.06	11.834	
		(- 0.29, - 0.43, 0.82, 0.25)	12.029	-	11.355	$\bar{D}_s^* \eta_b$
		(- 0.69, 0.31, - 0.26, 0.60)	12.097	-	11.539	$B_s \bar{B}_c$
(0.21, 0.84, 0.51, 0.02)		12.144	-	11.761		
$(sc\bar{c}\bar{b})$	2^+	(0.63, - 0.13, - 0.07, 0.76)	12.179	-	11.837	
		1.00	8.831	- 0.57	8.432	$\bar{D}_s^* B_c^*$
	1^+	1.00	8.840	- 0.57	8.566	
		(0.25, - 0.22, 0.60, - 0.57, 0.40, - 0.22)	8.720	- 0.14	8.288	$\bar{D}_s B_c^*$
		(- 0.18, 0.45, 0.67, 0.39, 0.12, 0.37)	8.772	- 0.41	8.368	
		(- 0.71, 0.21, - 0.07, - 0.62, - 0.11, 0.22)	8.799	- 0.63	8.408	
		(0.39, 0.64, - 0.38, - 0.21, 0.47, 0.16)	8.814	- 0.08	8.499	
	0^+	(- 0.11, - 0.31, - 0.19, 0.28, 0.77, - 0.05)	8.837	- 0.13	8.531	
		(0.23, - 0.46, - 0.06, - 0.10, 0.03, 0.86)	8.860	- 0.33	8.551	
		(- 0.17, - 0.63, 0.75, 0.13)	8.692	-	8.220	$\bar{D}_s B_c$
(0.81, - 0.29, 0.03, - 0.52)		8.762	-	8.375		
	(0.20, 0.72, 0.66, - 0.06)	8.799	-	8.488		
	(0.53, - 0.04, - 0.04, 0.85)	8.873	-	8.561		

state contains two states $(\phi_2\chi_1, \phi_1\chi_1)$ and the 1^+ state forms six mixed states $c_1\phi_2\chi_2 + c_2\phi_2\chi_4 + c_3\phi_2\chi_5 + c_4\phi_1\chi_2 + c_5\phi_1\chi_4 + c_6\phi_1\chi_5$ in the subspace $\{\phi_2\chi_2, \phi_2\chi_4, \phi_2\chi_5, \phi_1\chi_2, \phi_1\chi_4, \phi_1\chi_5\}$. Additionally, the 0^+ state forms the mixed states, $c_1\phi_2\chi_3 + c_2\phi_2\chi_6 + c_3\phi_1\chi_3 + c_4\phi_1\chi_6$, in the subspace $\{\phi_2\chi_3, \phi_2\chi_6, \phi_1\chi_3, \phi_1\chi_6\}$.

The computed masses and other properties of the tetraquark states are listed in Table 5. With their masses exceeding the two-meson thresholds, the triply heavy tetraquark $sc\bar{c}\bar{b}$ can decay to the channels $B_s^* J/\psi, B_s J/\psi, \bar{D}_s^* B_c^*, B_s^* \eta_c, \bar{D}_s^* B_c, B_s \eta_c, \bar{D}_s B_c^*$ and $\bar{D}_s \bar{B}_c$, as depicted in Fig. 6. The state $sb\bar{c}\bar{b}$ can decay to $B_s^* \bar{B}_c^*, B_s^* \bar{B}_c, B_s \bar{B}_c, B_s \bar{B}_c^*, \bar{D}_s^* \Upsilon, \bar{D}_s^* \eta_b, \bar{D}_s \Upsilon$ or $\bar{D}_s \eta_b$. Both of the tetraquarks $sc\bar{c}\bar{b}$ and $sb\bar{c}\bar{b}$ can be the candidates of the scattering states, as noted in Table 5.

4 Summary

In this work, we employ the MIT bag model which incorporates chromomagnetic interactions and enhanced binding energy to systematically study the masses and other prop-

erties of all triply heavy tetraquarks $(qQ_1\bar{Q}_2\bar{Q}_3)$ in their ground states. The variational analysis is applied to compute the masses, magnetic moments and charge radii of all strange and nonstrange (ground) states of triply heavy tetraquarks. Our computation indicates that all of these triply heavy tetraquark states are above their two-meson thresholds and can decay to their two-meson final states via strong interaction. We observe that the tetraquark states in configuration $6_c \otimes \bar{6}_c$ are usually heavier than that in $\bar{3}_c \otimes 3_c$ about 50 – 150 MeV for the same quantum number J^P , with exception for all $J^P = 1^+$ states with one multiplet in the middle of two others in the sense of the mass order. Furthermore, the mass splitting between them becomes smaller when more bottom quarks are involved. By the way, we estimate the relative decay widths of two-meson final states of the triply heavy tetraquarks and predict the primary decay channels for each of them. We hope that our prediction helps to find the triply heavy tetraquarks during experimental search in the future.

There are some scattered states among the tetraquark states $(sQ\bar{Q}\bar{Q}', nQ\bar{Q}\bar{Q}')$ which is based on the numerical evaluation of the I -th decay channel weight $|c_I|^2$. When $|c_I|^2$

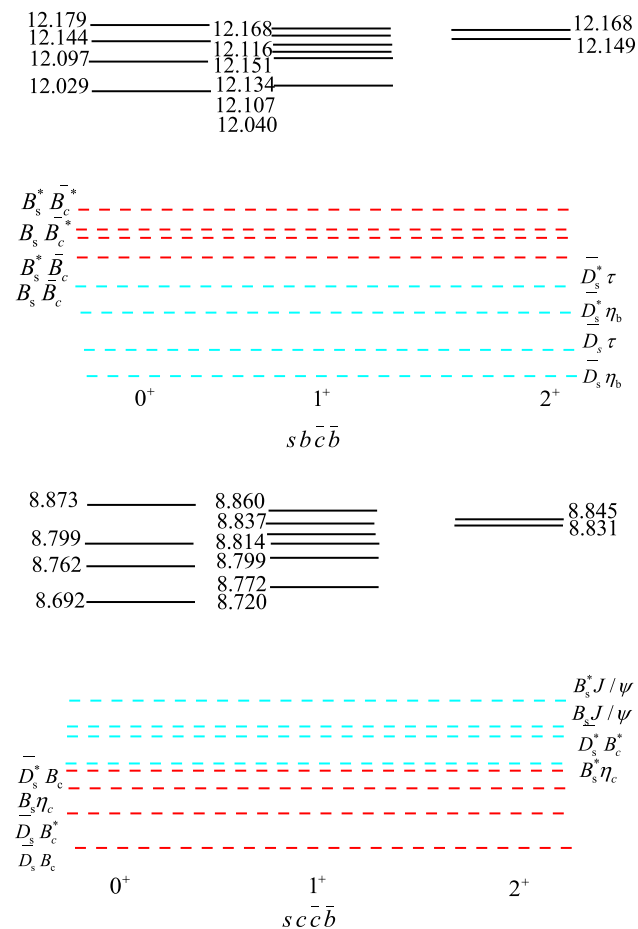


Fig. 6 Mass spectra(GeV, the solid lines) of the tetraquarks $sb\bar{c}\bar{b}$ and $sc\bar{c}\bar{b}$, with the meson-meson thresholds (GeV) plotted in dotted lines

tends to be close to unity, the tetraquark state turns out to be a scattering state, for which the decay and width computation are considered.

Acknowledgements D. J thanks Xue-Qian Li for discussions. D. J is supported by the National Natural Science Foundation of China under the no. 12165017.

Data Availability Statement This manuscript has associated data in a data repository. [Authors’ comment: Data are available upon request by contacting the corresponding author Duojie Jia].

Code Availability Statement This manuscript has associated code/software in a data repository. [Authors’ comment: Codes are available upon request by contacting the corresponding author Duojie Jia].

Open Access This article is licensed under a Creative Commons Attribution 4.0 International License, which permits use, sharing, adaptation, distribution and reproduction in any medium or format, as long as you give appropriate credit to the original author(s) and the source, provide a link to the Creative Commons licence, and indicate if changes were made. The images or other third party material in this article are included in the article’s Creative Commons licence, unless indicated otherwise in a credit line to the material. If material is not included in the article’s Creative Commons licence and your intended

use is not permitted by statutory regulation or exceeds the permitted use, you will need to obtain permission directly from the copyright holder. To view a copy of this licence, visit <http://creativecommons.org/licenses/by/4.0/>. Funded by SCOAP³.

Appendix A

In Eq. (6) of the MIT bag model, the rational function $F(x_i, x_j)$ is given by [44].

$$F(x_i, x_j) = \left(x_i \sin^2 x_i - \frac{3}{2} y_i\right)^{-1} \left(x_j \sin^2 x_j - \frac{3}{2} y_j\right)^{-1} \left\{-\frac{3}{2} y_i y_j - 2x_i x_j \sin^2 x_i \sin^2 x_j + \frac{1}{2} x_i x_j [2x_i \text{Si}(2x_i) + 2x_j \text{Si}(2x_j) - (x_i + x_j) \text{Si}(2(x_i + x_j)) - (x_i - x_j) \text{Si}(2(x_i - x_j))]\right\}, \tag{A1}$$

with $y_i = x_i - \cos(x_i)\sin(x_i)$. Here, the running strong coupling $\alpha_s(R)$ is defined as [36],

$$\alpha_s(R) = \frac{0.296}{\ln[1 + (R(0.281 \text{ GeV}))^{-1}]}, \tag{A2}$$

in which the bag radii R depends upon a dimensionless parameter $x_i = x_i(mR)$ via a transcendental equation.

$$\tan x_i = \frac{x_i}{1 - m_i R - (m_i^2 R^2 + x_i^2)^{1/2}}. \tag{A3}$$

Appendix B

The matrix elements in the CMI (3) can be evaluated via the following relations

$$\langle \lambda_i \cdot \lambda_j \rangle_{nm} = \sum_{\alpha=1}^8 Tr \left(c_{in}^\dagger \lambda^\alpha c_{im} \right) Tr \left(c_{jn}^\dagger \lambda^\alpha c_{jm} \right), \tag{B1}$$

$$\langle \sigma_i \cdot \sigma_j \rangle_{xy} = \sum_{\alpha=1}^3 Tr \left(\chi_{ix}^\dagger \sigma^\alpha \chi_{iy} \right) Tr \left(\chi_{jx}^\dagger \sigma^\alpha \chi_{jy} \right), \tag{B2}$$

where (n, m) and (x, y) refer to the indices of the color and spin states, respectively, i and j refer to quarks or antiquarks. Here, c_{in} stand for the color bases (color wavefunctions) of the quark(antiquark) i , and χ_{ix} stand for the spin bases of the quark(antiquark) i .

Based on formulas (B1) and the color wavefunctions in Sect. 2.2, one can compute all color factors for the normal hadrons (mesons and baryons) addressed in this work. For instance, the color factors is

$$\langle \lambda_1 \cdot \lambda_2 \rangle = -\frac{16}{3}, \tag{B3}$$

for the quark-antiquark in meson with the wave function (ϕ^M), and the color factor is

$$\langle \lambda_1 \cdot \lambda_2 \rangle = \langle \lambda_1 \cdot \lambda_3 \rangle = \langle \lambda_2 \cdot \lambda_3 \rangle = -\frac{8}{3}, \quad (\text{B4})$$

for quark pairs in the baryon with (ϕ^B).

For tetraquarks with two color configurations (ϕ_1^B, ϕ_2^B) in the zero-order approximation, the color factors for them are

$$\begin{aligned} \langle \lambda_1 \cdot \lambda_2 \rangle = \langle \lambda_3 \cdot \lambda_4 \rangle &= \begin{bmatrix} \frac{4}{3} & 0 \\ 0 & -\frac{8}{3} \end{bmatrix}, \\ \langle \lambda_1 \cdot \lambda_3 \rangle = \langle \lambda_2 \cdot \lambda_4 \rangle &= \begin{bmatrix} -\frac{10}{3} & 2\sqrt{2} \\ 2\sqrt{2} & -\frac{4}{3} \end{bmatrix}, \\ \langle \lambda_1 \cdot \lambda_4 \rangle = \langle \lambda_2 \cdot \lambda_3 \rangle &= \begin{bmatrix} -\frac{10}{3} & -2\sqrt{2} \\ -2\sqrt{2} & -\frac{4}{3} \end{bmatrix}, \end{aligned} \quad (\text{B5})$$

which are 2×2 matrices in the subspace spanned by the base wavefunctions (ϕ_1^T, ϕ_2^T). Here, base ϕ_1^T corresponds to the $\mathbf{6}_c \otimes \bar{\mathbf{6}}_c$ color configuration while ϕ_2^T corresponds to the $\bar{\mathbf{3}}_c \otimes \mathbf{3}_c$ color configuration.

References

- R.L. Workman et al. [Particle Data Group], Review of particle physics. PTEP **2022**, 083C01 (2022)
- M. Ablikim et al., Confirmation of a charged charmoniumlike state. Phys. Rev. D **092006**(2015). [arXiv:1509.01398](#) [hep-ex]
- M. Ablikim et al., Observation of a charged charmoniumlike structure. Phys. Rev. Lett. **112**, 132001 (2014). [arXiv:1308.2760](#) [hep-ex]
- M. Ablikim et al., Observation of a charged charmoniumlike structure. 242001 (2013). [arXiv:1309.1896](#) [hep-ex]
- M. Ablikim et al., Observation of a near-threshold structure in the K^+ recoil-mass Spectra. Phys. Rev. Lett. **126**, 102001 (2021)
- R. Aaij et al., Observation of new resonances decaying. Phys. Rev. Lett. **127**, 082001 (2021). [arXiv:2103.01803](#) [hep-ex]
- K. Chilikin et al. [Belle], Phys. Rev. D **90**(11), 112009 (2014). [arXiv:1408.6457](#) [hep-ex]
- K. Chilikin et al. [Belle], Experimental constraints on the spin and parity of the $Z(4430)94^+$. Phys. Rev. D **88**, 074026 (2013). [arXiv:1306.4894](#) [hep-ex]
- M.J. Yan, F.Z. Peng, M. Sánchez Sánchez, M. Pavon Valderrama, Axial meson exchange and the $Z_c(3900)$ and $Z_{cs}(3985)$ resonances as heavy hadron molecules. Phys. Rev. D **104**, 114025 (2021). [arXiv:2102.13058](#) [hep-ph]
- C. Deng, S.L. Zhu, Phys. Rev. D **105**(5), 054015 (2022). [arXiv:2112.12472](#) [hep-ph]
- M. Ablikim et al. [BESIII], Phys. Rev. Lett. **110**, 252001 (2013). [arXiv:1303.5949](#) [hep-ex]
- Z.Q. Liu et al. [Belle], Phys. Rev. Lett. **110**, 252002 (2013). [Erratum: Phys. Rev. Lett. **111**, 019901 (2013)]. [arXiv:1304.0121](#) [hep-ex]
- R. Aaij et al. [LHCb], Sci. Bull. **65**(23), 1983–1993 (2020). [arXiv:2006.16957](#) [hep-ex]
- I. Polyakov, [on behalf of LHCb Collaboration], Talk at the Euro. Phys. Soc. Conference on High Energy Physics (2021)
- L. Maiani, F. Piccinini, A.D. Polosa, V. Riquer, Diquark-antidiquark states with hidden or open charm. Phys. Rev. D **71**, 014028 (2005). [arXiv:hep-ph/0412098](#)
- W. Park, S.H. Lee, Color spin wave functions of heavy tetraquark states. Nucl. Phys. A. **925**, 02.008 (2014). [arXiv:1311.5330](#) [hep-ph]
- M.N. Anwar, J. Ferretti, E. Santopinto, Spectroscopy of the hidden-charm. Phys. Rev. D **98**, 094015 (2018). [arXiv:1805.06276](#) [hep-ph]
- A. Nils, From the deuteron to deusons, an analysis of deuteron-like meson-meson bound states. Zeitschrift Physik C Particles and Fields, vol. 61 (1994). [arXiv:1707.09575](#) [hep-ph]
- N.A. Trnqvist, Heavy-quark symmetry implies stable heavy tetraquark mesons $Q_i Q_j \bar{q}_k \bar{q}_l$. Phys. Lett. B **590** (2004). [arXiv:hep-ph/0402237](#)
- E.S. Swanson, Short range structure in the X(3872). Phys. Lett. B **588** (2004). [arXiv:hep-ph/0311229](#)
- C. Hanhart, Y.S. Kalashnikova, A.E. Kudryavtsev, A.V. Nefediev, Phys. Rev. D **76**, 034007 (2007). [arXiv:0704.0605](#) [hep-ph]
- F. Aceti, R. Molina, E. Oset, Phys. Rev. D **86**, 113007 (2012). [arXiv:1207.2832](#) [hep-ph]
- R. Chen, X. Liu, Y.-R. Liu, S.-L. Zhu, Predictions of the hidden-charm molecular states with the four quark components. Eur. Phys. J. C. **76** (2016). [arXiv:1511.03439](#) [hep-ph]
- S.-L. Zhu, The possible interpretations of Y(4260). Phys. Lett. B. **625** (2005). [arXiv:hep-ph/0507025](#)
- A. Esposito, A. Pilloni, A.D. Polosa, Hybridized tetraquarks. Phys. Lett. B **758** (2016). [arXiv:1603.07667](#) [hep-ph]
- M. Karliner, J.L. Rosner, Quark-level analogue of nuclear fusion with doubly heavy baryons. Phys. Rev. Lett. **551**, 24289 (2017). [arXiv:1708.02547](#) [hep-ph]
- E.J. Eichten, C. Quigg, Heavy-quark symmetry implies stable heavy tetraquark mesons $Q_i Q_j \bar{q}_k \bar{q}_l$. Phys. Rev. Lett. **119**, 202002 (2017). [arXiv:1707.09575](#) [hep-ph]
- D. Meng-Lin, W. Chen, X.-L. Chen, S.-L. Zhu, Phys. Rev. D **87**, 014003 (2013). [arXiv:1209.5134](#) [hep-ph]
- S. Fleck, J.M. Richard, Baryons with double charm. Prog. Theor. Phys. **82**, 760–774 (1989)
- D. Ebert, R.N. Faustov, V.O. Galkin, A.P. Martyanenko, Semileptonic decays of doubly heavy baryons in the relativistic quark model. Phys. Rev. D **70**, 014018 (2004). [Erratum: Phys. Rev. D **77**, 079903 (2008)]. [arXiv:hep-ph/0404280](#)
- W. Roberts, M. Pervin, Heavy baryons in a quark model. Int. J. Mod. Phys. A **23**, 2817–2860 (2008). [arXiv:0711.2492](#) [nucl-th]
- C. Albertus, E. Hernandez, J. Nieves, J.M. Verde-Velasco, Static properties and semileptonic decays of doubly heavy baryons in a nonrelativistic quark model. Eur. Phys. J. A **32**, 183–199 (2007). [Erratum: Eur. Phys. J. A **36**, 119 (2008)]. [arXiv:hep-ph/0610030](#)
- F. Giannuzzi, Doubly heavy baryons in a Salpeter model with AdS/QCD inspired potential. Phys. Rev. D **79**, 094002 (2009). [arXiv:0902.4624](#) [hep-ph]
- A. Bernotas, V. Simonis, Mixing of heavy baryons in the bag model calculations. Lith. J. Phys. Tech. Sci. **48**, 127 (2008). [arXiv:0801.3570](#) [hep-ph]
- M.Z. Liu, Y. Xiao, L.S. Geng, Magnetic moments of the spin-1/2 doubly charmed baryons in covariant baryon chiral perturbation theory. Phys. Rev. D **98**, 014040 (2018). [arXiv:1807.00912](#) [hep-ph]
- D.H. He, K. Qian, Y.B. Ding, X.Q. Li, P.N. Shen, Evaluation of spectra of baryons containing two heavy quarks in bag model. Phys. Rev. D **70**, 094004 (2004). [arXiv:hep-ph/0403301](#)
- M. Karliner, J.L. Rosner, Baryons with two heavy quarks: masses, production, decays, and detection. Phys. Rev. D **90**, 094007 (2014). [arXiv:1408.5877](#) [hep-ph]
- H. Mutuk, Eur. Phys. J. C **83**(5), 358 (2023). <https://doi.org/10.1140/epjc/s10052-023-11526-7>. [arXiv:2305.03358](#) [hep-ph]
- L. Meng, Y.K. Chen, Y. Ma, S.L. Zhu, Phys. Rev. D **108**(11), 114016 (2023). <https://doi.org/10.1103/PhysRevD.108.114016>. [arXiv:2310.13354](#) [hep-ph]

40. X. Liu, Y. Tan, D. Chen, H. Huang, J. Ping, Phys. Rev. D **107**(5), 054019 (2023). <https://doi.org/10.1103/PhysRevD.107.054019>. [arXiv:2205.08281](https://arxiv.org/abs/2205.08281) [hep-ph]
41. Q.F. Lü, D.Y. Chen, Y.B. Dong, E. Santopinto, Phys. Rev. D **104**(5), 054026 (2021). <https://doi.org/10.1103/PhysRevD.104.054026>. [arXiv:2107.13930](https://arxiv.org/abs/2107.13930) [hep-ph]
42. T. Guo, J. Li, J. Zhao, L. He, Phys. Rev. D **105**(1), 014021 (2022). <https://doi.org/10.1103/PhysRevD.105.014021>. [arXiv:2108.10462](https://arxiv.org/abs/2108.10462) [hep-ph]
43. Y. Cui, X.L. Chen, W.Z. Deng, S.L. Zhu, HEPNP **31**, 7–13 (2007). [arXiv:hep-ph/0607226](https://arxiv.org/abs/hep-ph/0607226)
44. T.A. DeGrand, R.L. Jaffe, K. Johnson, J.E. Kiskis, Masses and other parameters of the light hadrons. Phys. Rev. D **12**, 2060 (1975)
45. W.-X. Zhang, X. Hao, D. Jia, Masses and magnetic moments of hadrons with one and two open heavy quarks: heavy baryons and tetraquarks. Phys. Rev. D **104**, 114011 (2021). [arXiv:2109.07040](https://arxiv.org/abs/2109.07040) [hep-ph]
46. X.-Z. Weng, W.-Z. Deng, S.-L. Zhu, Triply heavy tetraquark states. Phys. Rev. D **105**, 034026 (2022). [arXiv:2109.05243](https://arxiv.org/abs/2109.05243) [hep-ph]
47. A. Chodos, R.L. Jaffe, K. Johnson, C.B. Thorn, Baryon structure in the bag theory. Phys. Rev. D **10**, 2599 (1974)